

# Electrochemical Oxidation of Polyaniline in Nonaqueous Electrolytes: "In Situ" Raman Spectroscopic Studies

M. Lapkowski,<sup>†,‡</sup> K. Berrada,<sup>§</sup> S. Quillard,<sup>\*,§</sup> G. Louarn,<sup>§</sup> S. Lefrant,<sup>§</sup> and A. Pron<sup>||,⊥</sup>

*Institute of Physical Chemistry and Technology of Polymers, Silesian Technical University, 44100 Gliwice, Poland, Department of Textile Engineering and Environmental Sciences, Technical University of Lodz, Bielsko-Biala Campus, 43300 Bielsko-Biala, Plac Fabryczny, Poland, Laboratoire de Physique Cristalline, Institut des Matériaux, 2 rue de la Houssinière, 44072 Nantes Cedex 03, France, Department of Materials Science and Ceramics, Academy of Mining and Metallurgy, Mickiewicza 30, 30059 Cracow, Poland, and Department of Chemistry, Technical University of Warsaw, Noakowskiego 3, 00664 Warsaw, Poland*

Received July 18, 1994; Revised Manuscript Received November 8, 1994\*

**ABSTRACT:** Spectroelectrochemical behavior of polyaniline in nonaqueous electrolytes has been studied by Raman spectroscopy using two excitation lines: blue (457 nm) and infrared (1064 nm). It has been demonstrated that in the electrolytic solution consisting of tetrabutylammonium tetrafluoroborate/diphenyl phosphate/acetonitrile both oxidation processes (oxidation of leucoemeraldine to emeraldine and emeraldine to pernigraniline) can be investigated by Raman spectroscopy. The blue excitation line is very insensitive to the oxidation and protonation changes occurring during the first oxidation process and reveals only the reduced segments of polyaniline chains. However in the second oxidation process significant changes in the Raman spectra occur, consistent with the formation of pernigraniline units accompanied by deprotonation of the polymer. No Raman spectrum can be recorded for the most reduced form of polyaniline using the infrared excitation line. However gradual oxidation of the polymer results in the appearance of the Raman bands characteristic of the oxidized units which are strongly resonantly enhanced. The infrared line is extremely sensitive toward the existence of protonated segments and allows for direct monitoring of the deprotonation processes occurring during the second oxidation process (i.e. the oxidation of emeraldine to pernigraniline).

## Introduction

In recent years, several research reports devoted to various aspects of the chemistry and physics of polyaniline have been published. This scientific interest was stimulated mainly by the fact that polyaniline exhibits extremely interesting properties which make this polymer suitable for a variety of technological applications.

Recent preparation of solution<sup>1</sup> and thermally processable<sup>2</sup> conducting polyaniline enables the applications of polyaniline-based composites and blends in antistatic coatings, transparent electrodes,<sup>3</sup> etc. Finally, several applications of this polymer in electrochemistry and spectroelectrochemistry have been reported.<sup>4-6</sup>

Polyaniline exhibits rather complicated spectroelectrochemical behavior because, depending on the potential and electrolyte used, it can exist in a variety of oxidation and protonation states which distinctly differ in their spectral features.

The existence of chromophore groups at practically each oxidation state of polyaniline results in a strong resonance effect clearly observed in Raman spectroscopic studies. Thus in Raman spectra of polyaniline the observed lines are not only dependent on the oxidation and protonation state of the polymer but also on the position of the excitation line with respect to the observed electronic transitions.

Several papers have been published on Raman spectroelectrochemical behavior of polyaniline.<sup>7-11</sup> However in the vast majority of these studies aqueous electrolytes were used.

Cyclic voltammograms of polyaniline recorded in aqueous acidic media usually show two redox couples associated with redox interconversion between leucoemeraldine and emeraldine (the first couple) and between emeraldine and pernigraniline (the second redox couple).<sup>12</sup> At the potentials of the second oxidation peak polyaniline is unstable in aqueous solutions and undergoes degradation of a hydrolytic nature. Therefore reliable spectroelectrochemical data can be obtained only for the potentials lower than the onset of the second oxidation peak, i.e. below 700 mV vs SCE.

In nonaqueous electrolytes polyaniline can be polarized at potentials exceeding the second oxidation peak without significant degradation. Raman spectroelectrochemical properties of polyaniline in nonaqueous electrolytes have previously been studied by Ueda et al.<sup>13</sup> However these authors limited themselves to the studies of the first redox process.

In this paper, we report "in situ" Raman spectroelectrochemical studies involving both redox processes. We also try to exploit the resonance Raman effect using two different excitation lines: blue (457 nm) and infrared (1064 nm).

## Experimental Section

All reagents used were purchased from Aldrich. Aniline (ACS reagent grade) was distilled prior to its use, tetrabutylammonium tetrafluoroborate (TBABF<sub>4</sub>) was vacuum dried, and acetonitrile (anhydrous) was used without further purification. All loading operations were carried out in a dry nitrogen atmosphere.

Polyaniline was synthesized voltammetrically in a three-electrode cell with platinum working and counter electrodes and an SCE reference. The polymerization medium consisted of 0.25 M solution of aniline in 1 M HCl. Successive layers of the polymer were deposited on the electrode by potential scanning between -200 and +700 mV vs SCE. The deposited

<sup>†</sup> Silesian Technical University.

<sup>‡</sup> Technical University of Lodz.

<sup>§</sup> Institut des Matériaux.

<sup>||</sup> Academy of Mining and Metallurgy.

<sup>⊥</sup> Technical University of Warsaw.

\* Abstract published in *Advance ACS Abstracts*, January 15, 1995.

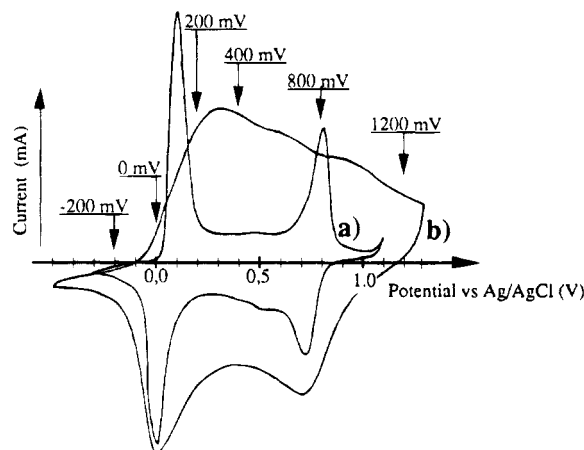


**Figure 1.** Cyclic voltammograms of polyaniline in (a) TBABF<sub>4</sub>/diphenyl phosphate/acetonitrile (scanning rate 50 mV/s) and (b) TBABF<sub>4</sub>/acetonitrile (scanning rate 50 mV/s).

film was then repeatedly rinsed with water and then with acetonitrile and finally dried under dynamic vacuum.

Cyclic voltammograms were recorded in a 0.2 M solution of tetrabutylammonium tetrafluoroborate (TBABF<sub>4</sub>) in acetonitrile which was acidified with diphenyl phosphate (concentration of the latter being 0.1 M). Diphenyl phosphate is known to protonate polyemeraldine base in nonaqueous media<sup>14</sup> and was added to facilitate proton exchange during electrochemical oxidation. Ag/AgCl was used as the reference electrode. The spectroelectrochemical cell used in all experiments has been described elsewhere.<sup>15</sup>

The same solution was used for the "in situ" Raman spectroelectrochemical studies. The spectra obtained with the excitation line from the visible range (457 nm) were recorded on a multichannel Jobin-Yvon T 64000 spectrometer connected to a CCD detector. For IR excitation (1064 nm) an FT Raman Bruker RFS 100 was used. The scattering signal was collected at 90° for  $\lambda_{\text{exc}} = 457$  nm. In FT Raman experiments a backscattering configuration was used.

## Results

In Figure 1a the cyclic voltammogram of polyaniline recorded in a nonaqueous medium of TBABF<sub>4</sub>/diphenyl phosphate/acetonitrile is presented. It should be stressed here that the addition of diphenyl hydrogen phosphate (the compound which greatly facilitates proton exchange between polyaniline and the electrolyte) improves the shape of the voltammogram (compare Figure 1a and 1b). Similarly, as in the case of aqueous electrolytes, two clearly separated and well-defined oxidation peaks can be distinguished. The reduction part of the voltammetric curve exhibits more complicated features and consists of at least three strongly overlapping peaks.

If no protonating agent is added to the electrolyte, broad, strongly overlapping and rather poorly defined oxidation peaks are observed in the cyclic voltammogram (Figure 1b). Of course spectroelectrochemical separation of both redox processes is in this case very difficult.

Raman spectra recorded for the polymer film polarized at selected potentials from the potential range covered by cyclic voltammetry are presented in Figures 2 and 3 for the excitation lines of 457 nm and 1064 nm, respectively.

In aqueous media, the blue (457 nm) line is not a very efficient probe for studying the spectroelectrochemical behavior of polyaniline.<sup>15</sup> Up to the onset of the second oxidation peak (i.e. to the limit of reversible oxidation in aqueous media) no significant changes due to the oxidation can be observed in Raman spectra. In non-

aqueous electrolytes however more information can be gained. The spectroelectrochemical features observed in this case can be briefly described as follows.

At  $E = -200$  mV (i.e. below the onset of the first oxidation), in the spectral range 1000–1650 cm<sup>-1</sup>, the spectrum consists of essentially two peaks at 1190 and 1622 cm<sup>-1</sup>, which are characteristic of C–H in plane bending and C–C stretching deformations in benzoid-type rings.<sup>16</sup> The increase of the polarization potential up to the onset of the second oxidation peak does not result in any significant change of the number and the positions of the observed peaks. However together with the first oxidation peak fluorescence appears and grows in intensity with increasing polarization potentials up to  $E = +600$  mV; then it decreases. For the clarity of Figure 2a, the Raman spectra are presented after the subtraction of the fluorescence. The spectrum recorded at  $E = -200$  mV is resonantly enhanced with respect to the others. Again for the clarity, this enhancement is not indicated in Figure 2a.

An abrupt change in Raman spectra coincides with the second oxidation wave. In particular, a strong peak grows at 1475 cm<sup>-1</sup>, which can be ascribed to nonprotonated quinoid-type segments.<sup>17</sup> At the same time, the single line at 1624 cm<sup>-1</sup> characteristic of C–C stretching deformations splits into two lines peaked at 1588 and 1629 cm<sup>-1</sup>, the former being characteristic of the C–C stretching in quinoid segments, whereas the latter is usually ascribed to C–C stretching deformation in benzoid rings.<sup>16</sup> A distinct peak at 1219 cm<sup>-1</sup> unobserved for lower potentials appears (C–N stretching deformations<sup>16</sup>). The peak due to C–H in-plane bending deformations (1172 cm<sup>-1</sup>) is being downshifted as compared to the spectra recorded at lower potentials, and its position is intermediate between those expected for benzoid and quinoid structures.

Very similar results are obtained for the "in situ" Raman spectroelectrochemical studies carried out in TBABF<sub>4</sub>/acetonitrile electrolyte without the admixture of diphenyl hydrogen phosphate. However, in this case, the second oxidation as probed by Raman spectroscopy starts at ca. 200 mV lower potential.

The use of the infrared excitation line ( $\lambda_{\text{exc}} = 1064$  nm) leads to totally different resonant behavior. At potentials below the onset of the first oxidation peak no spectrum with reasonable signal to noise ratio can be recorded. The resonant enhancement leading to clearly resolved spectra coincides with the first oxidation peak and remains approximately constant until the potential of the second oxidation is reached. Then, the intensity of the lines increases again. Since for comparative reasons, it is more convenient to present spectra with approximately the same intensity of the lines, the resonant enhancements were not shown in Figure 3.

As soon as they begin to appear, Raman spectra obtained with the use of  $\lambda_{\text{exc}} = 1064$  nm, exhibit features characteristic of the existence of oxidized units in the polymer. While the blue excitation line produces, at  $E = +200$  mV, only two Raman bands characteristic of the benzoid-type units, the FT Raman ( $\lambda_{\text{exc}} = 1064$  nm) spectrum shows, at the same potential, several lines characteristic of quinoid, semiquinoid, and benzoid structures (vide infra).

The increase of the polarization potential to  $E = +800$  mV produces a gradual increase of the bands at ca. 1235 and 1320 cm<sup>-1</sup>. Simultaneously, the bands in the vicinity of 1570–1620 cm<sup>-1</sup> usually ascribed to –C–C

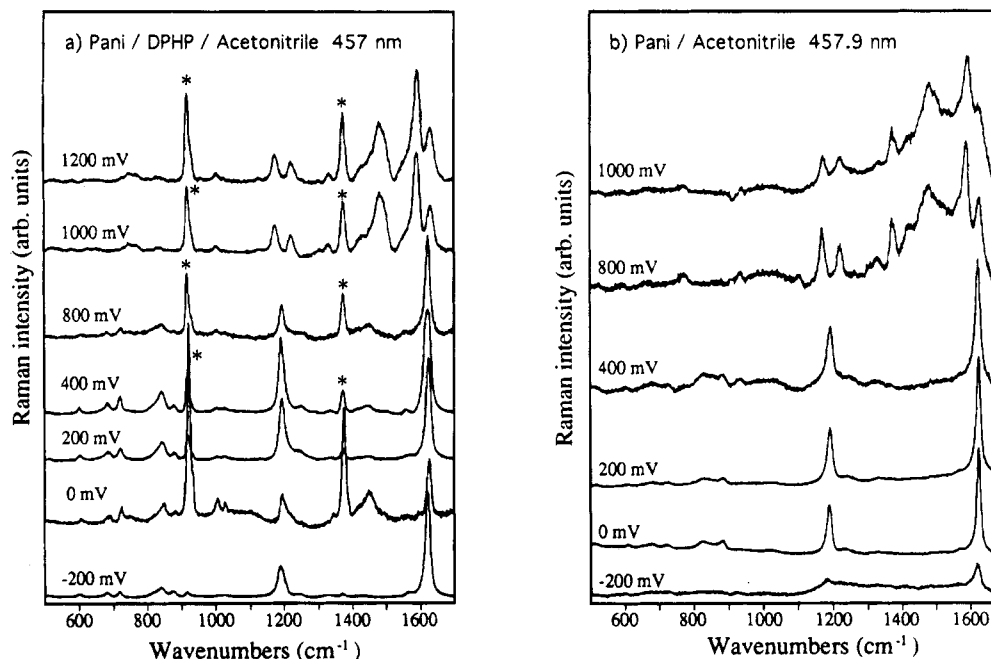


**Figure 2.** Raman spectra of polyaniline obtained with the use of the excitation line  $\lambda_{\text{exc}} = 457.9$  nm (a) in TBABF<sub>4</sub>/diphenyl phosphate/acetonitrile electrolyte (\*: acetonitrile Raman bands) and (b) in TBABF<sub>4</sub>/acetonitrile electrolyte.

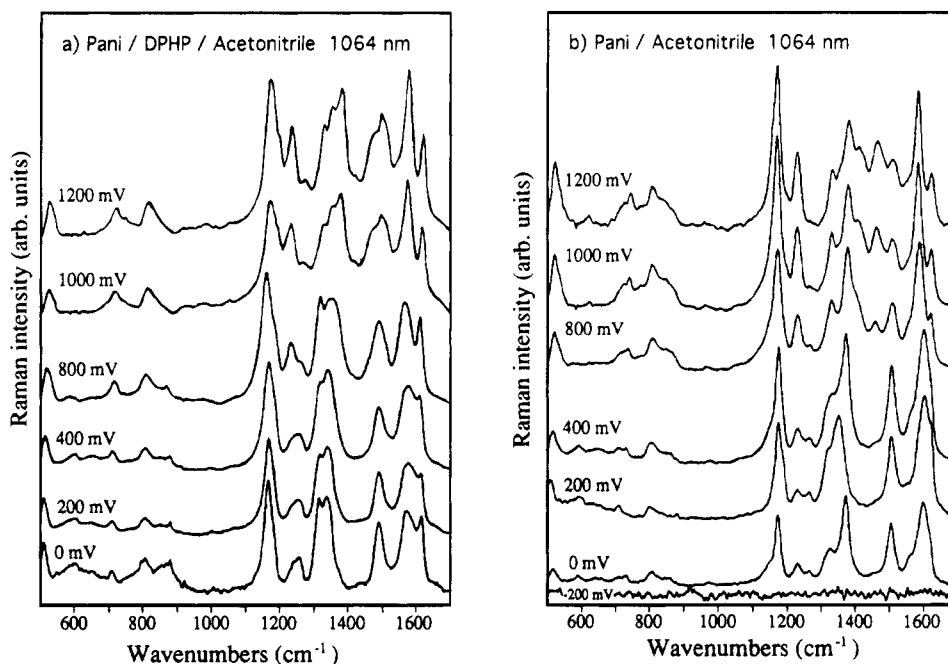


**Figure 3.** Raman spectra of polyaniline obtained with the use of the excitation line  $\lambda_{\text{exc}} = 1064$  nm (a) in TBABF<sub>4</sub>/diphenyl phosphate/acetonitrile electrolyte and (b) in TBABF<sub>4</sub>/acetonitrile electrolyte.

stretchings in various structural units (quinoid, semi-quinoid, benzoid) narrow and become better resolved.

At the potentials of the second oxidation peak ( $E = 900\text{--}1200$  mV vs Ag/AgCl) further significant changes occur in the  $1300\text{--}1400$   $\text{cm}^{-1}$  spectral range. A new peak appears at ca.  $1380$   $\text{cm}^{-1}$  and grows in intensity at the expense of the  $1320$   $\text{cm}^{-1}$  peak. Simultaneously, a new band grows at ca.  $1470$   $\text{cm}^{-1}$  clearly visible as a shoulder of the  $1500$   $\text{cm}^{-1}$  peak.

Similarly, as in the case of the blue excitation line, in FT Raman spectroscopic signs of the second oxidation appear at lower potentials if no diphenyl hydrogen phosphate is added to TBABF<sub>4</sub>/acetonitrile electrolyte (compare Figure 3a,b). There exist however some spectroscopic differences between the film oxidized in

TBABF<sub>4</sub>/DHP/acetonitrile electrolyte and the one oxidized in the solution without the admixture of DHP. The C=N stretching deformations band at  $1462$   $\text{cm}^{-1}$  ascribed to the presence of quinoid units is more pronounced in the latter case and well-separated from the  $1500$   $\text{cm}^{-1}$  line. Also, out of three peaks in the spectral region characteristic of semiquinone radical structures ( $1300\text{--}1400$   $\text{cm}^{-1}$ ) two are blue shifted (to ca.  $1379$  and  $1408$   $\text{cm}^{-1}$ ).

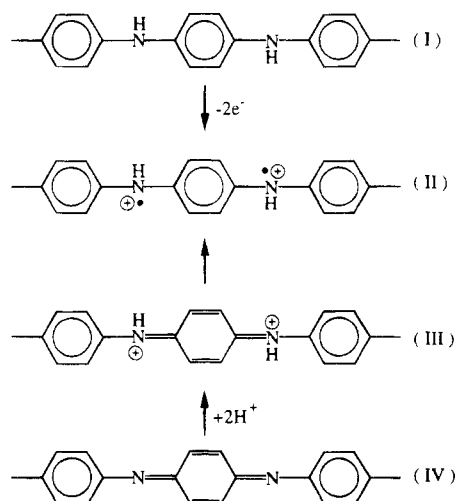
#### Discussion

In Table 1 calculated for leucoemeraldine and pernigraniline forms Raman active modes (taken from ref 18) are collected and compared with those observed experimentally in leucoemeraldine, pernigraniline, and emeraldine bases.

**Table 1. Experimentally Observed Raman Modes in Leucoemeraldine, Emeraldine, Pernigraniline Bases and Semiquinone-Radical Structure<sup>a</sup>**

| leucoemeraldine base |      | emeraldine base |          | pernigraniline base |      | semiquinone struct | description of vibrations    |
|----------------------|------|-----------------|----------|---------------------|------|--------------------|------------------------------|
| 457.9 nm             |      | 457.9 nm        | 647.1 nm | 647.1 nm            |      | 1064 nm            |                              |
| exp                  | calc | exp             | exp      | exp                 | calc | exp                |                              |
| 1618                 | 1620 | 1620            | 1618     | 1612                | 1614 | } $\approx 1590$   | C-C stretching <sup>8a</sup> |
| 1597                 | 1588 | 1551            | 1553     | 1553                | 1591 |                    | C-C stretching <sup>8b</sup> |
|                      |      | 1590            | 1586     | 1579                | 1581 |                    | C=C stretching Q             |
|                      |      | 1486            | 1480     | 1480                | 1496 |                    | C=N stretching (X-sens)      |
|                      |      | 1420            | 1420     | 1418                | 1417 |                    | C-C stretching Q             |
|                      |      | (1330)          |          |                     |      | 1507               |                              |
|                      |      |                 |          |                     |      | 1330-1350          | protonated structure         |
| 1219                 | 1217 | $\approx 1220$  | 1217     | 1215                | 1207 | 1260               | C-N stretching (X-sens)      |
| 1181                 | 1168 | 1186            |          |                     | 1171 | 1170               | C-H bending <sup>9a</sup>    |
|                      |      | 1162            | 1160     | 1157                | 1155 |                    | C-H bending Q                |
| 868                  | 878  | 880             | 870      |                     | 880  |                    | ring deformation B           |
| 820                  |      | 828             | 826      |                     |      |                    | amine def (X-sens)           |
|                      |      |                 | 788      | 788                 | 800  | 810                | ring deformation Q           |
|                      |      | 720             | 750      | 749                 | 704  | 714                | imine deformation            |
| 667                  | 669  | 668             |          |                     |      |                    | amine def (X-sens)           |
|                      |      |                 |          |                     | 612  |                    | ring deformation Q           |
| 603                  | 610  |                 | 640      |                     | 604  |                    | ring deformation B           |

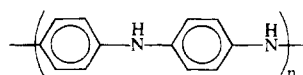
<sup>a</sup> For comparison calculated Raman modes for leucoemeraldine and pernigraniline bases are presented.<sup>18</sup>

**Scheme 1**

In addition to the modes expected for the above mentioned basic forms of polyaniline, modes ascribed to protonated (salt) forms of polyaniline may be present. Protonated polyaniline can be obtained either by electrochemical oxidation of leucoemeraldine base or by protonation of emeraldine according to Scheme 1.

It is postulated that protonated polyaniline exhibits a semiquinone radical type of structure (II)<sup>19</sup> created either by direct oxidation of I or by protonation of IV followed by an internal redox process which transforms III into IV. In the semiquinone radical units the C-N bond order is intermediate between those of amine >C-N< and imine >C=N- groups. The peaks due to C-N stretching deformations are therefore expected between the positions of the amine group peaks (1220  $\text{cm}^{-1}$ ) and imine group ones (1470  $\text{cm}^{-1}$ ), i.e. in the 1300-1400  $\text{cm}^{-1}$  spectral region. These bands are diagnostic of semiquinone radical structure and do not appear in other forms of polyaniline.

In its most reduced state polyaniline exists as leucoemeraldine—a linear polymer consisting of para-substituted benzoid rings joined together by amine nitrogens, e.g.



In the 1000-1650  $\text{cm}^{-1}$  spectral range leucoemeraldine should give rise to three major Raman bands associated with C-C stretching deformations in benzoid rings (ca. 1620  $\text{cm}^{-1}$ ), C-H in-plane bending deformations (ca. 1180  $\text{cm}^{-1}$ ), and >C-N< stretching deformations (ca. 1230  $\text{cm}^{-1}$ ). In the spectrum of the polymer recorded at the potential  $E = -500$  mV vs Ag/AgCl using the 457 nm excitation line, all three expected bands are present, although the peak due to C-N stretching is weak and broad. In FT Raman ( $\lambda_{\text{exc}} = 1064$  nm) no spectrum can be recorded, indicating that at  $E = -500$  mV no segments in the polymer chain exist which are in resonance with the excitation line.

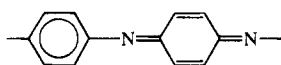
This observation can be correlated with the UV-vis-near IR spectrum of polyaniline recorded at  $E = -500$  mV.<sup>20</sup> Reduced polyaniline exhibits one absorption band in the UV region whose tail extends to the visible.<sup>20</sup> Thus, using the blue ( $\lambda_{\text{exc}} = 457$  nm) line we are in preresonance conditions. On the other hand, the absorption in red and near IR regions is negligible and no resonant Raman effect can be produced with  $\lambda_{\text{exc}} = 1064$  nm. In general no Raman spectrum can be recorded with the infrared excitation line before the first oxidation starts (i.e. below  $E = 200$  mV vs Ag/AgCl). This is in striking contrast with the results obtained in aqueous electrolytes where clear spectra were recorded for potentials significantly lower than the onset of the first oxidation peak.<sup>15</sup> The existence of oxidized segments in reduced polyaniline was rationalized by the reactive nature of leucoemeraldine, which could be locally oxidized even if polarized at negative potentials. It may be therefore concluded that the oxidation of leucoemeraldine in nonaqueous media caused by external contaminants with oxidizing properties is slower than in the aqueous ones.

The blue ( $\lambda_{\text{exc}} = 457$  nm) excitation line produces Raman spectra which are extremely insensitive to the oxidation and protonation phenomena associated with the first oxidation peak. Up to  $E = 800$  mV the spectrum essentially does not change and only the bands due to the presence of reduced units are registered. Only at  $E = 800$  mV can a weak and broad line peaked at 1325  $\text{cm}^{-1}$ , which is characteristic of the protonated semiquinone radical structure, be seen. For aqueous electrolytes the same behavior is observed. However in aqueous media no second oxidation process can be

studied because of the hydrolytic instability of pernigraniline.

In TBABF<sub>4</sub>/DHP/acetonitrile solution significant changes in the spectra coincide with the onset of the second oxidation. One can easily notice correlated growth of three peaks characteristic of unprotonated quinoid rings, namely at 1218 cm<sup>-1</sup> (>C=N< stretching), at 1475 cm<sup>-1</sup> (>C=N stretching), and at 1589 cm<sup>-1</sup> (-C=C- stretching in the quinoid ring).

In reality the spectrum recorded above  $E = 800$  mV vs Ag/AgCl closely resembles that of pernigraniline base prepared by chemical oxidation.<sup>21</sup> This observation is consistent with spontaneous deprotonation of polyaniline occurring during the oxidation of emeraldine to pernigraniline observed by Troise Frank and Denuault<sup>22</sup> in scanning electrochemical microscopy experiments. At the potentials of the second oxidation peak, semiquinone radical segments, undetectable by Raman spectroscopy with  $\lambda_{\text{exc}} = 457$  nm, become unstable and deprotonate to give oxidized units in their basic form:



Thus the co-existence of benzoid and quinoid segments above  $E = 800$  mV vs Ag/AgCl is clearly manifested in Raman spectra obtained with  $\lambda_{\text{exc}} = 457$  nm.

In contrast to the blue line, the infrared ( $\lambda_{\text{exc}} = 1064$  nm) excitation line is extremely sensitive toward the presence of semiquinone radical structures. Moreover the FT Raman spectrum cannot be registered until some of these groups appear in the polymer. The position of the lines ascribed to semiquinone radical segments depends on the extent of electron delocalization. In oligomers where this delocalization is limited they appear at higher energies (1380–1400 cm<sup>-1</sup>).<sup>13</sup> Within the potentials of the first redox process, the oxidation of polyaniline gives rise to two broad strongly overlapping peaks with maxima at ca. 1320 and ca. 1350 cm<sup>-1</sup>. The lower energy peaks grow with the increase of the potential up to  $E = 800$  mV vs Ag/AgCl. The co-existence of two peaks indicates that the distribution of semiquinone radical structures is not uniform and various domains with different electron delocalizations may be present.

Strong sensitivity of FT Raman toward the semiquinone radical structures is not unexpected. Conducting, protonated polyaniline exhibits electronic transitions which extend to near IR improving resonance conditions in the case of  $\lambda_{\text{exc}} = 1064$  nm. Similarly, as in the case of the blue excitation line, spectral changes occurring in FT Raman, at the potentials of the second oxidation, are consistent with the oxidation-induced deprotonation. In conducting polyaniline semiquinone radical structures dominate. The formation of these structure leads to the uniformization of the chain because in ideal poly-(semiquinone radical) all rings and nitrogens should be chemically equivalent. As a result at the potentials of the stability of semiquinone radical structures, the observed Raman bands are intermediate between those expected for the benzoid and quinoid structures. At the potentials of the second oxidation process, quick spectroscopic differentiation between quinoid and benzoid segments occurs. In particular the lines attributed to -C=C- stretching in benzoid and quinoid rings narrow and separate (1623 and 1580 cm<sup>-1</sup>). At the same time the lines attributed to >C=N- and >C=N- stretching deformations appear at 1235 and 1470 cm<sup>-1</sup>, respec-

tively, and grow in intensity as the expense of the "semiquinone radical" line (1320 cm<sup>-1</sup>).

Such behavior reflects deprotonation induced by transformation of emeraldine into pernigraniline. As expected with increasing potential, the intensity of the "protonation bands" decreases relatively to the other bands. However they exist even at the potential of  $E = 1200$  mV vs Ag/AgCl, indicating that at the experimental conditions used the deprotonation of pernigraniline is not complete. The bands associated with residual protonation are shifted toward higher energies, showing that electrons are more localized in these structures.

## Conclusions

To summarize, we have studied the spectroelectrochemical behavior of polyaniline in nonaqueous solutions using Raman spectroscopy with the blue (457 nm) and infrared (1064 nm) excitation lines. The obtained results allow for the formulation of the following conclusions.

(i) The admixture of diphenyl hydrogen phosphate (DHP) with TBABF<sub>4</sub>/acetonitrile electrolyte greatly improves the cyclic voltammetric behavior of polyaniline in nonaqueous solutions. DHP is known to protonate polyaniline even in nonpolar and weakly polar solvents, and its addition facilitates proton exchange phenomena occurring during the oxidation of polyaniline. As a result, in their oxidation part, cyclic voltammograms obtained in TBABF<sub>4</sub>/DHP/acetonitrile solutions look like those obtained in aqueous acidic solutions. Good separation of the oxidation peaks in cyclic voltammetry allows for good differentiation between spectroelectrochemical phenomena associated with each oxidation.

(ii) Within the potentials of the first oxidation (leucoemeraldine to emeraldine) the use of  $\lambda_{\text{exc}} = 457$  nm leads to the spectra which are very insensitive to the oxidation and protonation state of polyaniline and look like the spectra of leucoemeraldine. However upon the onset of the second oxidation peak significant spectral changes occur, consistent with the formation of pernigraniline base.

(iii) No spectrum of totally reduced polyaniline can be obtained with the use of the infrared excitation line (1064 nm). The formation of partially oxidized segments at the onset of the first oxidation peak allows for the registration of the Raman spectra. The infrared line is extremely sensitive toward the existence of protonated segments and allows for direct monitoring of the deprotonation processes occurring during the second oxidation process (i.e. the oxidation of emeraldine to pernigraniline).

## References and Notes

- (1) Cao, Y.; Smith, P.; Heeger, A. J. *Synth. Met.* **1992**, *48*, 91.
- (2) Pron, A.; Laska, J.; Osterholm, J. E.; Smith, P. *Polymer* **1993**, *34*, 4235.
- (3) Gustafsson, G.; Cao, Y.; Treacy, G. M.; Klavetter, F.; Colaneri, N.; Heeger, A. J. *Nature* **1992**, *353*, 477.
- (4) Morita, M. J. *Polym. Sci. B: Polym. Phys.* **1994**, *32*, 231; *Macromol. Chem. Phys.* **1994**, *195*, 609.
- (5) Jelle, B. P.; Hagen, G. J. *Electrochem. Soc.* **1993**, *140*, 3560.
- (6) Kalaji, M.; Nyholm, L.; Peter, L. M. J. *Electroanal. Chem. Interfacial Electrochem.* **1992**, *325*, 269.
- (7) Kuzmany, H.; Sariciftci, N. S. *Synth. Met.* **1987**, *18*, 353.
- (8) Furukawa, Y.; Hana, T.; Hyodo, Y.; Harada, I. *Synth. Met.* **1986**, *16*, 189.
- (9) Monkman, A. P. *Conjugated Polymeric Materials*; NATO ASI Series 182; Kluwer: Boston, 1990; p 273.
- (10) Bernard, M. C.; Cordoba-Torresi, S.; Hugot-LeGoff, A. *Sol. Energy Mat. Sol. Cells* **1992**, *25*, 225.

- (11) Hugot-Le Goff, A.; Bernard, M. C. *Synth. Met.* **1993**, *60*, 115.
- (12) Huang, W. S.; Humphrey, B. D.; MacDiarmid, A. G. *J. Chem. Soc., Faraday Trans.* **1986**, *82*, 2385.
- (13) Ueda, F.; Mukai, K.; Harada, I.; Nakajima, T.; Kawagoe, T. *Macromolecules* **1990**, *23*, 4925.
- (14) Laska, J.; Pron, A.; Lefrant, S. *J. Polym. Sci., Polym. Chem. Ed.*, in press.
- (15) Quillard, S.; Berrada, K.; Louarn, G.; Lapkowski, M.; Lefrant, S.; Pron, A. *New J. Chem.*, in press.
- (16) Quillard, S.; Louarn, G.; Buisson, J. P.; Lefrant, S.; Masters, J.; MacDiarmid, A. G. *Synth. Met.* **1992**, *49-50*, 525.
- (17) Furukawa, Y.; Ueda, F.; Hyodo, Y.; Harada, I.; Nakajima, T.; Kawagoe, T. *Macromolecules* **1988**, *21*, 1297.
- (18) Quillard, S.; Louarn, G.; Lefrant, S. *Phys. Rev. B* **1994**, *50*, 12496.
- (19) Wnek, G. E. *Synth. Met.* **1986**, *15*, 213.
- (20) Genies, E. M.; Lapkowski, M. *J. Electroanal. Chem. Interfacial Electrochem.* **1987**, *220*, 67.
- (21) Quillard, S.; Louarn, G.; Buisson, J. P.; Lefrant, S.; Masters, J.; MacDiarmid, A. G. *Synth. Met.* **1993**, *55-57*, 475.
- (22) Troise Frank, M. H.; Denuault, G. *J. Electroanal. Chem. Interfacial Electrochem.* **1993**, *354*, 331.

MA9411641